MRS Communications

https://doi.org/10.1557/s43579-024-00548-1

MRS Communications

Additive Manufacturing of Functional and Smart Composites
Research Letter

Additively manufactured 3D short carbon fiber scaffold for thermoset composites

Chunyan Zhang, and Kelvin Fu, Center for Composite Materials, University of Delaware, Newark, DE 19716, USA; Department of Mechanical Engineering, University of Delaware, Newark, DE 19716, USA

Address all correspondence to Chunyan Zhang at **zcy@udel.edu** and Kelvin Fu at **kfu@udel.edu**

(Received 12 February 2024; accepted 14 March 2024)

Abstract

Short-fiber-reinforced polymer composites offer advantages, like flexibility in complex geometries and cost-effectiveness, but typically exhibit lower mechanical properties because of the random orientation of short fibers. In this work, a novel process utilizing shear force to create 3D scaffold with customized fiber alignment for the manufacturing of short carbon fibers (SCF)-reinforced thermoset composites has been presented. The Computed tomography test confirmed the alignment of the SCF along printing directions. The results demonstrate that the aligned SCF-reinforced epoxy composites exhibited a 190% improvement in tensile strength and 388% improvement in tensile modulus compared to neat epoxy.

Introduction

The industrial application of short-fiber (a few micrometers—3 mm in length)-reinforced polymer composites (SFRPCs) has seen a significant increase, particularly in the construction and automotive industries. This growth can be attributed to their advantages, including the ability to fabricate components with complicated geometries, cost-effectiveness, and a high production rate by manufacturing techniques such as injection molding.[1–5] It is worth noting the SFRPCs usually exhibit lower mechanical properties due to the random orientation of the short fibers. To improve the mechanical properties of the SFRPCs, achieving a high degree of fiber alignment along the loading direction is a key trend.[6–8] Gillespie et al.[6] developed a thin-film material Tailored Universal Feedstock for Forming (TuFF) that leverages hydrodynamic assistance to achieve highly aligned SCF (3 mm in length) membrane for composites manufacturing. This method yielded composites with a 57% fiber volume fraction and a remarkable ~95% fiber alignment, achieving a tensile strength of 2668 MPa in the direction of short-fiber alignment, comparable to continuous fiber composites. These findings highlight the potential of achieving significant mechanical properties in SFRPCs with controlled fiber alignment, paving the way for advancements in material design and performance optimization. Therefore, it is of great significance to develop a general method to align SCF in a preferred direction.

Various strategies have been employed to orient fibers in a preferred direction during SFRPCs processing, including shear force,[9–12] pneumatic means, magnetic and electrical field assistance, compression molding,[13] and hydrodynamic or flow assistance.[8,14] Among these, shear force is a simple and effective approach and has been employed to enhance fiber alignment and improve composite mechanical properties. Shear alignment in extrusion 3D printing process leverages the inherent flow characteristics of the molten filament to manipulate fiber alignment during deposition. By strategically controlling printing parameters, like nozzle size, printing speed, and layer height, extrusion 3D printing can induce shear forces and flow patterns within the micro-filament, influencing the orientation of embedded short fibers. This approach enables the creation of customized 3D structures with intricate geometry and precisely controlled fiber alignment directions, potentially leading to optimized mechanical properties and performance tailored to specific applications. While extrusion 3D printing with short fibers in thermoplastics was initially explored, thermosetting polymers offer several advantages. These advantages stem from the strong, irreversible chemical bonds formed after curing, compared to the weaker van der Waals forces in thermoplastics. However, this curing process needs to happen quickly during 3D printing, which is a challenge.[15–18] To address this, developing a process that separates the printing and curing steps is crucial. This would allow for more flexibility and control in fabricating complex 3D structures with fibers.

In this work, we present a novel process, utilizing shear force to align short fibers for the creation of 3D scaffold structure, for producing SCF-reinforced thermoset composites. This innovative process comprises three key steps which are extrusion 3D printing of thermoplastic part with tailored 3D structures and fiber orientations, carbonization of the printed structures for robust scaffolds composed of aligned SCF, and impregnating the 3D SCF scaffold with a chosen thermoset resin. Computed tomography (CT) analysis revealed the alignment of SCF along the printing directions within the 3D scaffold structure. SCF/epoxy composites were successfully produced using this process and their tensile performance was compared with that of neat epoxy. The tensile strength and

modulus of the SCF/epoxy composites are 97.88 MPa and 7.61 GPa, respectively. The incorporation of aligned SCF significantly enhanced the mechanical properties of the composites, with tensile strength increasing by 190% and modulus increasing by 388% compared to neat epoxy (tensile strength: 51.73 MPa, tensile modulus: 1.96 GPa). Detailed characterization, including filament analysis, fiber orientation, and distribution of the fiber in the epoxy matrix, are presented to underscore the potential of this newly developed thermoset composite manufacturing method. This approach empowers the creation of composites with tailored functionality and intricate structures for diverse applications.

Materials and methods

Materials

Short carbon fibers (140 μm in length and 5 μm in diameter) were provided by CarbonForm. Polylactic acid granules (LX175) and dichloromethane (DCM) were purchased from Filabot (Barre, Vermont, USA) and Sigma-Aldrich (St. Louis, State of Missouri, USA), respectively. Epoxy 4600 resin and harder were purchased from Fibre Glast (Brookville, Ohio, USA), mixed at a 10:2 weight ratio as per the manufacturer's recommendation.

Materials characterization

The morphology of the extruded SCF/PLA filament and SCF/epoxy composite was characterized using a scanning electron microscope (Auriga 60 CrossBeam). Thermogravimetric analysis (TGA) was used to determine the PLA content in the composite feedstock under Nitrogen condition for up to 420°C with a heating rate of 10°C/min. Differential scanning calorimetry (DSC) was employed on a TA discovery DSC with cooling capability to analyze thermal behavior from 30 to 210°C at 20°C/min under nitrogen. The alignment of SCF was examined by SEM and computed tomography (CT). Tensile testing was performed at room temperature on an Instron 5985 tester equipped with a 10-kN load cell at a displacement rate of 1 mm/min.

Results and discussion

The manufacturing process of SCF-reinforced thermoset composites involves printing a thermoplastic part that incorporates a PLA-bonded architecture. In the printing process, due to the shear force between the SCF/PLA composite filament and the nozzle wall, SCF spontaneously forms an aligned structure along the printing direction. Subsequent carbonization is employed to decompose the PLA component, resulting in a SCF scaffold. This SCF part comprises a three-dimensional structure composed of aligned fibers and contains pores/channels. Following this, epoxy is infiltrated into the SCF scaffold to prepare thermoset composites [Fig. 1(a)]. Figure 1(b) is a photo of the prepared SCF/epoxy composite for tensile testing. SEM conducted on the inner structure of the composite reveals the alignment of the SCF in the epoxy matrix [Fig. 1(c)]. Mechanical property of the SCF/epoxy was measured to evaluate their potential application in aerospace and automotive. We tested the tensile properties of neat epoxy and SCF/epoxy samples with load parallel to the printing directions. A minimum of three coupons were tested for each material at room temperature, and the average results are reported [Fig. 1(d)]. As observed, the neat epoxy sample exhibited an average longitudinal tensile strength of 51.73 MPa and a longitudinal elastic modulus of 1.96 GPa, respectively. The SCF/epoxy sample exhibited an average longitudinal tensile strength of 97.88 MPa and a longitudinal elastic modulus of 7.61 GPa, respectively. Compared to the tensile property of neat epoxy, the longitudinal tensile strength and modulus of the SCF/epoxy composite exhibited a 190% and 388% improvement, respectively.

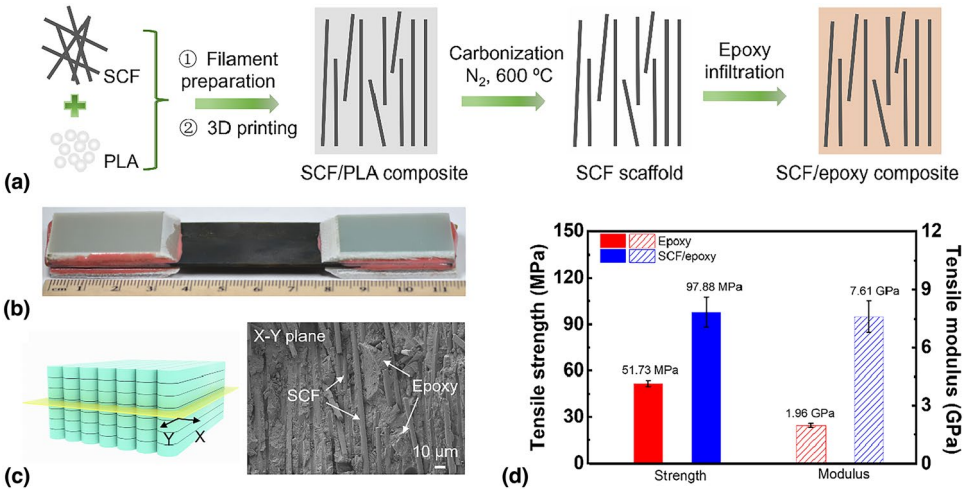

Figure 1. Additive manufacturing of 3D thermoset composites. (a) Schematic illustration of the manufacturing process for 3D thermoset composites from SCF. (b) Photo of the prepared SCF/epoxy sample for tensile testing. (c) SEM image of the SCF/epoxy composite, along with the corresponding schematic diagram illustrating the positioning of where the SEM image was taken. (d) Tensile strength and modulus of neat epoxy and SCF/epoxy composite.

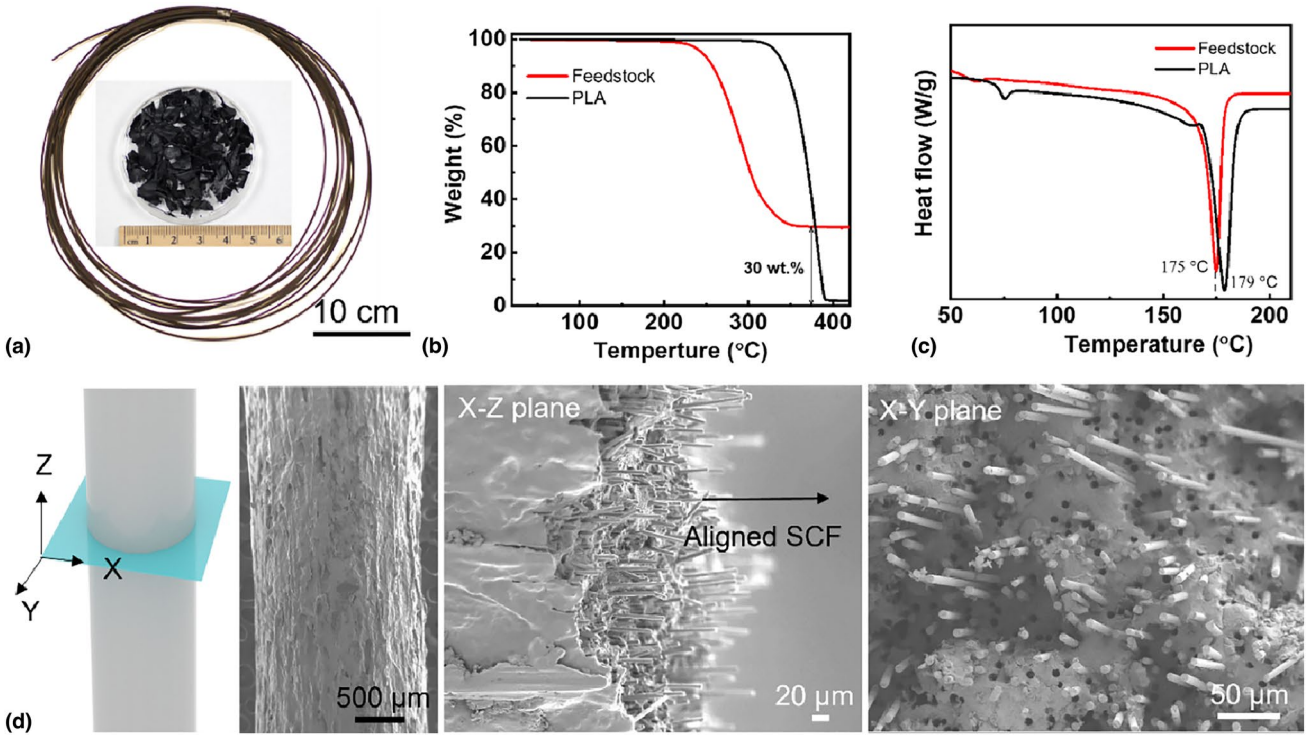

Figure 2. Characterization of filament composite. (a) Schematic of manufacturing of SCF/PLA composite filament. Inset shows the composite feedstock. (b) TGA of neat PLA and SCF composite feedstock in nitrogen environment. (c) DSC curves of neat PLA and composite, showing the tiny drift of the melting temperature after adding 30-wt.% additives in the PLA. (d) Schematic diagram of planes of SCF/PLA filament and corresponding SEM images of surface and fractured surfaces in SCF/PLA filament, showing the alignment of SCF along the filament extrusion direction, as highlighted with arrow.

Figure 2 presents thermal analysis and morphology characterization of the composite filament obtained using the prepared feedstock and extruding process. The composite feedstock was created by mixing reinforcement and PLA at a weight ratio of 30/70. Specifically, PLA granules were first dissolved in a DCM solvent under thorough stir until PLA fully dissolved. SCF powder was then added and fully dispersed in the PLA/DCM solution while maintaining continuous stirring. This viscous solution was dried overnight to remove excess DCM solvent, obtaining SCF/PLA membrane. The membrane was manually cut into small pieces and then extruded to form a filament. A commercial single-screw extruder was applied to prepare the filaments with 30-wt.% loading of SCF in PLA polymer matrix. The extrusion temperature was maintained at 190°C and the extrusion speed was carefully controlled to form a continuous and uniform filament with a diameter of 1.75 ± 0.01 mm. Figure 2(a) shows a 5-m long SCF-reinforced filament with an average diameter of 1.75 m, suitable for extrusion-based 3D printing. The composition of filament was confirmed through TGA, revealing 30-wt.% additives in PLA [Fig. 2(b)]. The 30-wt.% SCF in PLA is the highest loading achievable in our laboratory to produce continuous and uniform filaments without fracture during printing. To explore higher loadings, we prepared and characterized a 40-wt.% SCF/PLA filament (Figure S1). However, during testing of its printability on our printer, we observed that this filament became more brittle, leading to filament fracture when fed into the printer gear during the printing process. Before printing, DSC was conducted to obtain the melting temperature of the 30-wt.% SCF/PLA composite feedstock. As shown in Fig. 2(c), the melting temperature of the neat PLA and composite feedstock are 179℃ and 175℃, respectively. This indicates that the addition of 30-wt% reinforcement in the PLA did not significantly affect the melting temperature, suggesting that the printing temperature should be higher than 175℃. The morphology of the filament was characterized by SEM [Fig. 2(d)]. The SEM image further confirms the diameter of the filament, which is 1.75 mm. The side-view (X–Z plane) SEM image of the fracture surface reveals the orientation of SCF along the extruding direction. Additionally, the cross-section (X–Y plane) SEM images (Figure S2) of the filament indicate the uniform distribution of SCF in the composite filaments. These characteristics are beneficial for the extrusion 3D printing process and enhance the performance of printed parts.

Extrusion 3D printing offers the capability for tailoring reinforcement architecture in polymer composites through the manipulation of reinforcement. During the printing process, the molten polymer filament experiences shear forces as it exits the

heated nozzle and interacts with the printing platform, critically influencing the alignment of SCF along the printing directions [Fig. 3(a)]. The effects of printing temperature and speed on the SCF alignment were evaluated by SEM characterization of the SCF structures. The SCF structure printed at 10 mm/s exhibits weaker alignment compared to those prepared at other speeds [Fig. 3(b)], highlighting the influence of printing speed on SCF alignment. To evaluate the effect of printing parameters (temperature and speed) on the mechanical properties of the composites, tensile testing was conducted on 3D-printed SCF/PLA composites (Figure S3). The SCF-reinforced composite prepared at a printing speed of 10 mm/s exhibits a lower tensile strength compared to those prepared at 30 and 50 mm/s [Figure S3(C)]. This is likely due to weaker fiber alignment in the printing direction at lower printing speed.[19] The SCF-reinforced composite prepared at 230°C showed a lower tensile strength compared to those at 190 and 210°C [Figure S3(D)], likely due to PLA decomposition at the higher temperature. These findings highlight the importance of optimizing printing parameters for maximizing the mechanical properties of SCF-reinforced composites. The build plate was set at 30°C and coated with glue before printing. In this work, a printing temperature of 190°C and a printing speed of 30 mm/s were selected (detailed printing parameters are provided in Table S1). The ability to orient SCF was employed to manufacture a SCF architecture with 0° and 90° fiber orientations. The printed structure was carbonized under nitrogen (N_2) by heating it from room temperature to 600°C and holding it for 30 min to completely remove the PLA matrix. It was then cooled to room temperature at a rate of 5°C/min, resulting in a SCF scaffold. Figure 3(c) shows the printed SCF/PLA structure before and after carbonization process, showing the structure was maintained after PLA removal. SEM conducted on the scaffold indicates that the alignment of the SCF is preserved after PLA removal [Fig. 3(d)]. To further illustrate the capability of aligning SCF along different printing directions, a sample was prepared with orientations

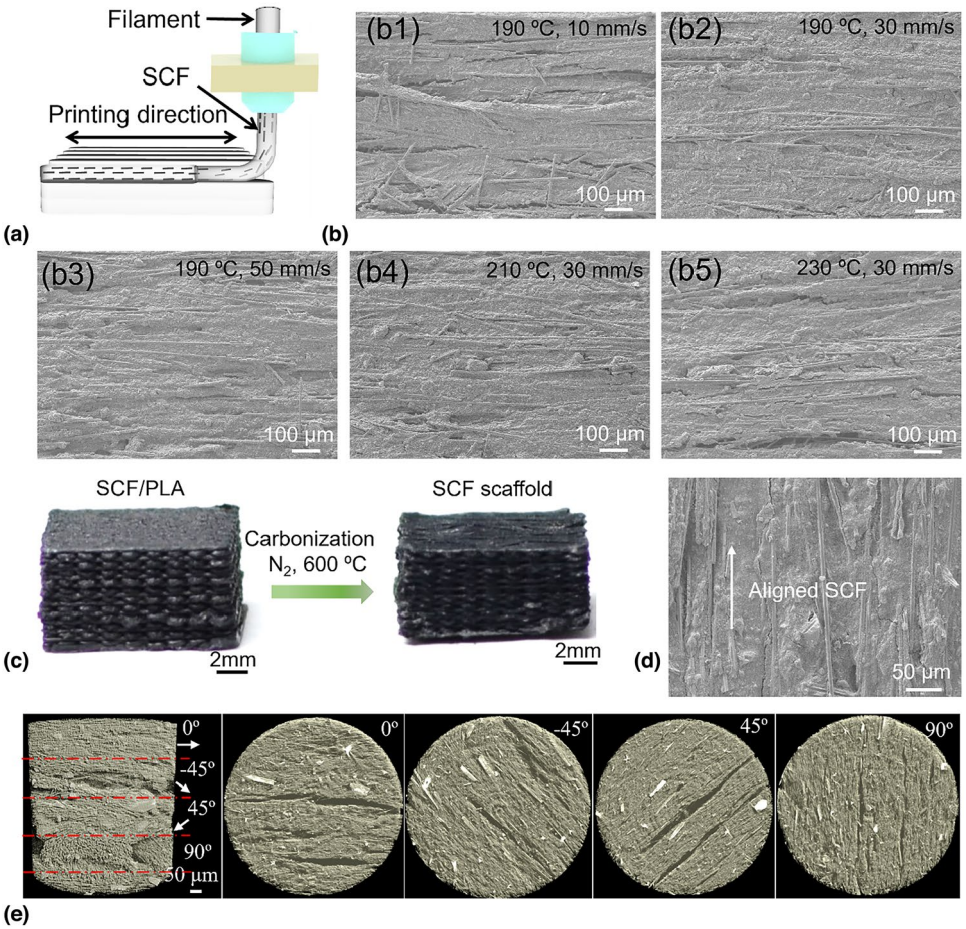

Figure 3. SCF scaffolds formation and its characterization. (a) Schematic illustration of the alignment of SCF induced by extrusion 3D printing. (b) SEM images of the SCF structures prepared at various parameters (b1) 190°C, 10 mm/s, (b2) 190°C, 30 mm/s, (b3) 190°C, 50 mm/s, (b4) 210°C, 30 mm/s, and (b5) 230°C, 30 mm/s showing that the printing speed has a significant effect on the alignment of SCF. (c) The comparison of the SCF/PLA part and SCF scaffold before and after carbonization demonstrates the preservation of the structure after PLA removal. (d) SEM image of the resulting SCF scaffold. (e) The 3D-reconstructed X-ray CT image of the SCF scaffold showing an aligned SCF arrangement along the printing directions.

of 0°, − 45°, 45°, and 90°. Subsequent CT analysis of the SCF scaffold [Fig. 3(e)] confirms successful alignment of the fibers along their respective printing directions within the 3D structure. The height or size of the SCF scaffold that could be produced using this method was evaluated by calculating that the maximum height that a SCF scaffold with a cross-section of 100 mm by 100 mm can support. The result revealed that the maximum height was 1.11 km (Figure S4; detailed calculation is provided in supporting materials). The theoretical calculation confirms that our method could potentially fabricate tall and large size parts.

SCF/epoxy composites were fabricated by infiltrating the 3D SCF scaffold with liquid epoxy using the vacuum-assisted resin transfer molding (VARTM) technique. Tensile properties of the neat epoxy and SCF/epoxy were measured. The exemplary stress–strain curves of neat epoxy and SCF/epoxy samples are shown in Fig. 4(a). All of the specimens failed immediately after the tensile stress reached its maximum. No obvious yield point was found in the curves. The tensile strength values were obtained by considering the peak load values divided by the cross-section area of the specimens. Tensile modulus values were obtained by linear regression of stress versus strain curves in the range of 0.2%-0.4%. The incorporation of SCF increased the tensile strength from 51.73 ± 1.97 MPa (epoxy) to 97.88 ± 9.55 MPa (SCF/epoxy) and modulus from 1.96 ± 0.11 GPa (epoxy) to 7.61 ± 0.80 GPa (SCF/epoxy), respectively. The addition of SCF enhances the ultimate tensile strength and modulus. After testing, the fracture surface of the SCF/epoxy specimen was gold sputtered and then observed with a SEM to analyze the dispersion of the fiber and understand the failure mechanisms. SEM image [Fig. 4(b)] indicates the uniform dispersion of SCF in the epoxy matrix and existence of the voids in the composites as highlighted with white arrows. It is seen that the surfaces of the fibers were not coated with the epoxy and most of the fiber pulled out, which can be attributed to the poor interfacial adhesion between the fiber and matrix. Moreover, the stresses during tensile test are not high enough to cause fiber failure after matrix fracture. The SCF weight ratio was determined based on the TGA results [Fig. 4(c)], revealing ~ 34-wt.% (24.5 vol.%) SCF in the finished composites. Subsequently, we attempted to fabricate 34-wt.% SCF/epoxy composites with random SCF orientations (details are provided in supporting materials). However, the resulting material exhibits

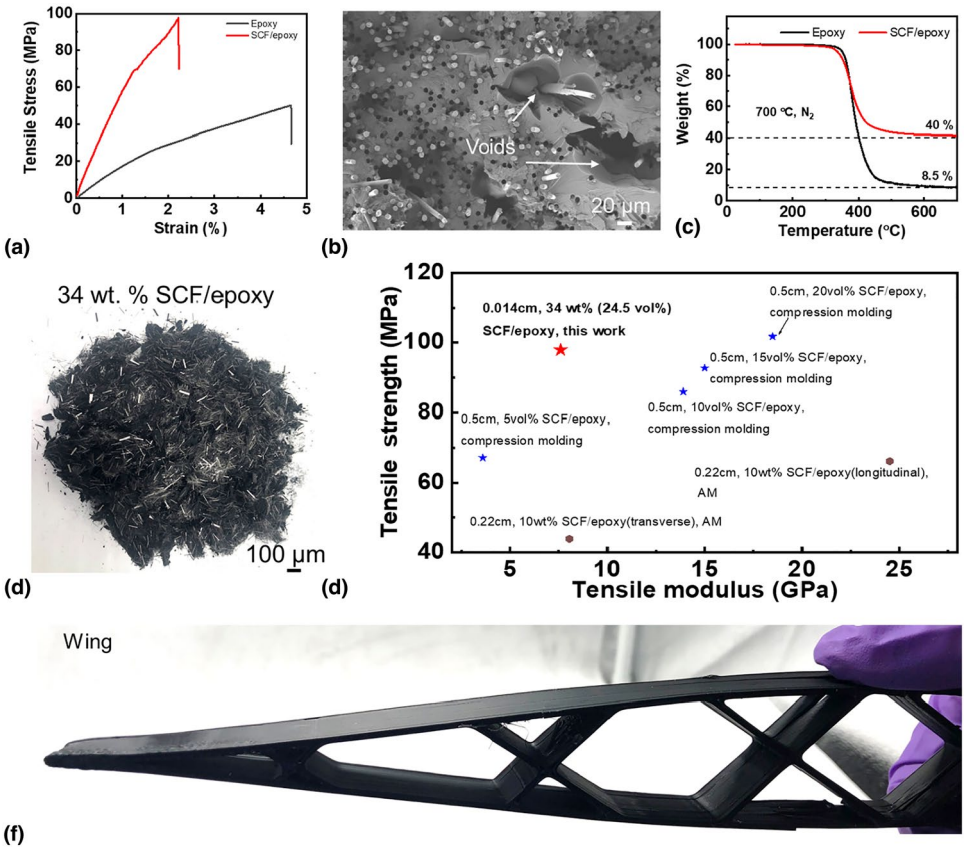

Figure 4. Characterization of SCF/epoxy composite and representative 3D part. (a) Representative tensile stress–strain curves of neat epoxy and SCF/epoxy composite. (b) SEM of the SCF/epoxy after tensile test. (c) TGA of the epoxy and SCF/epoxy composite. (d) Photo of the prepared 34-wt.% SCF/epoxy composites with random SCF orientations. (e) Comparison of tensile strength and modulus of SCF/epoxy composites with representative short carbon fiber composites prepared by other methods.[4,9] AM represents additive manufacturing. (f) Photo of representative 3D part prepared by this strategy.

a powder-like structure [Fig. 4(d)] and could not be formed into the desired shape for mechanical testing. We compared the tensile strength and modulus of SCF/epoxy composites prepared by this method with those prepared by other methods [Fig. 4(e)]. It was observed that SCF/epoxy composites prepared with this strategy could achieve high tensile strength and fiber contents with shorter fiber length. In short-fiber composites, fiber length plays a critical role in determining their mechanical properties. A simple model for understanding this relationship is the concept of critical fiber length. This model suggests that when the fiber length exceeds the critical length, the fibers can effectively bridge across the matrix, distributing and transferring loads more efficiently, resulting in improved mechanical performance. The tensile strength of carbon fiber (Hexcel, Stamford, USA) varies between 4413 and 6826 MPa. Taking the carbon fiber and epoxy strength (51.73 MPa) as constant, the critical length (l_c) of SCF is calculated to be 369–571 μm according to:[20]

$$l_c = \sigma_r d\sqrt{3}/(2\sigma_m), \quad (1)$$

where d is the fiber diameter and σ_r and σ_m are the ultimate strengths of the reinforcement and the matrix, respectively. This suggests that mechanical properties can be further improved by increasing the fiber length to equal or greater than the critical length. Our process successfully fabricates 3D parts (wing) with intricate geometric features, as shown in Fig. 4(f). This capability is advantageous for applications requiring complex functionalities and intricate geometries, such as sports equipment, aerospace, and automotive.

Conclusion

This study demonstrated the fabrication of SCF/epoxy composites reinforced with aligned 3D SCF scaffolds. The aligned 3D SCF scaffolds were prepared by carbonizing 3D-printed SCF/PLA structures, where the shear force exerted by the printing nozzle effectively oriented the SCF along the printing direction. CT analysis confirmed the alignment of SCF along the printing directions within the 3D scaffold structure. This finding confirms the effectiveness of the proposed fabrication process in manipulating fiber orientation, which is crucial for achieving enhanced mechanical properties in the resulting composite. Compared to neat epoxy (tensile strength: 51.73 MPa, tensile modulus: 1.96 GPa), the incorporation of aligned SCF significantly enhanced the mechanical properties of the composites. Tensile strength increased by 190% to 97.88 MPa, while modulus showed a remarkable 388% increase to 7.61 GPa. These results highlight the effectiveness of using shear forces in extrusion 3D printing for aligning SCF and the potential of this approach for creating high-performance thermoset composites.

Acknowledgments

We thank Gerald Poirier for helping with the CT test.

Author contributions

CZ performed the main experiments, characterization, and manuscript writing. KF supervised the work and participated in the discussion of the research as well as writing the manuscript. All authors discussed the results and commented on the manuscript.

Funding

The information, data, or work presented herein were funded by the University of Delaware startup and Department of Energy (DoE) under grant DE-FE0032147.

Data availability

All data are available in the manuscript.

Declarations

Conflict of interest

The authors have no conflicts of interest to declare.

Supplementary Information

The online version contains supplementary material available at https://doi.org/10.1557/s43579-024-00548-1.

References

1. S. Mortazavian, A. Fatemi, Effects of fiber orientation and anisotropy on tensile strength and elastic modulus of short fiber reinforced polymer

composites. Compos. B Eng. **72**, 116–129 (2015). https://doi.org/10.1016/j.compositesb.2014.11.041
2. Z. Jia, T. Li, F.-p Chiang, L. Wang, An experimental investigation of the temperature effect on the mechanics of carbon fiber reinforced polymer composites. Compos. Sci. Technol. **154**, 53–63 (2018). https://doi.org/10.1016/j.compscitech.2017.11.015
3. S.-Y. Fu, B. Lauke, E. Mäder, C.-Y. Yue, X. Hu, Tensile properties of short-glass-fiber-and short-carbon-fiber-reinforced polypropylene composites. Compos. Part A Appl. Sci. Manuf. **31**, 1117 (2000)
4. C. Capela, S.E. Oliveira, J.A.M. Ferreira, Fatigue behavior of short carbon fiber reinforced epoxy composites. Compos. B Eng. **164**, 191–197 (2019). https://doi.org/10.1016/j.compositesb.2018.11.035
5. M. Eftekhari, A. Fatemi, On the strengthening effect of increasing cycling frequency on fatigue behavior of some polymers and their composites: experiments and modeling. Int. J. Fatigue **87**, 153–166 (2016). https://doi.org/10.1016/j.ijfatigue.2016.01.014
6. S. Yarlagadda, J. Deitzel, D. Heider, J. Tierney, J.W. Gillespie, Tailorable universal feedstock for forming (TUFF): overview and performance, in *SAMPE Conference Proceedings*, Charlotte, 2019
7. M.L. Longana, N. Ong, H.N. Yu, K.D. Potter, Multiple closed loop recycling of carbon fibre composites with the HiPerDiF (high performance discontinuous fibre) method. Compos. Struct. **153**, 271–277 (2016). https://doi.org/10.1016/j.compstruct.2016.06.018
8. H. Yu, K.D. Potter, M.R. Wisnom, A novel manufacturing method for aligned discontinuous fibre composites (high performance-discontinuous fibre method). Compos. Part A Appl. Sci. Manuf. **65**, 175–185 (2014). https://doi.org/10.1016/j.compositesa.2014.06.005
9. B.G. Compton, J.A. Lewis, 3D-printing of lightweight cellular composites. Adv. Mater. **26**, 5930–5935 (2014). https://doi.org/10.1002/adma.201401804
10. C. Zhang, B. Shi, J. He, L. Zhou, S. Park, S. Doshi, Y. Shang, K. Deng, M. Giordano, X. Qi, S. Cui, L. Liu, C. Ni, K.K. Fu, Carbon additive manufacturing with a near-replica "green-to-brown" transformation. Adv. Mater. (2023). https://doi.org/10.1002/adma.202208230
11. H. Guo, H. Zhao, H. Niu, Y. Ren, H. Fang, X. Fang, R. Lv, M. Maqbool, S. Bai, Highly thermally conductive 3D printed graphene filled polymer composites for scalable thermal management applications. ACS Nano **15**, 6917–6928 (2021). https://doi.org/10.1021/acsnano.0c10768
12. C. Zhang, K. Deng, X. Li, K.K. Fu, C. Ni, Thermally conductive 3D-printed carbon-nanotube-filled polymer nanocomposites for scalable thermal management. ACS Appl. Nano Mater. **6**, 13400–13408 (2023). https://doi.org/10.1021/acsanm.3c02067
13. T.A. Turner, N.A. Warrior, S.J. Pickering, Development of high value moulding compounds from recycled carbon fibres. Plast. Rubber Compos. (2010). https://doi.org/10.1179/174328910X12647080902295
14. David C. Guell, Alan L. Graham, Improved mechanical properties in hydrodynamically aligned, short-fiber composite materials. J. Compos. Mater. **30**, 2–12 (1996)
15. B. Wang, Z. Zhang, Z. Pei, J. Qiu, S. Wang, Current progress on the 3D printing of thermosets. Adv. Compos. Hybrid Mater. **3**, 462–472 (2020). https://doi.org/10.1007/s42114-020-00183-z/Published
16. M. Mahmoudi, S.R. Burlison, S. Moreno, M. Minary-Jolandan, Additive-free and support-free 3d printing of thermosetting polymers with isotropic mechanical properties. ACS Appl. Mater. Interfaces **13**, 5529–5538 (2021). https://doi.org/10.1021/acsami.0c19608
17. M. Ziaee, J.W. Johnson, M. Yourdkhani, 3D printing of short-carbon-fiber-reinforced thermoset polymer composites via frontal polymerization. ACS Appl. Mater. Interfaces **14**, 16694–16702 (2022). https://doi.org/10.1021/acsami.2c02076
18. Y. Ming, S. Zhang, W. Han, B. Wang, Y. Duan, H. Xiao, Investigation on process parameters of 3D printed continuous carbon fiber-reinforced thermosetting epoxy composites. Addit. Manuf. (2020). https://doi.org/10.1016/j.addma.2020.101184
19. J. Reinold, V. Gudžulić, G. Meschke, Computational modeling of fiber orientation during 3D-concrete-printing. Comput. Mech. **71**, 1205–1225 (2023). https://doi.org/10.1007/s00466-023-02304-z
20. H.A. Pierson, E. Celik, A. Abbott, H. de Jarnette, L. Sierra Gutierrez, K. Johnson, H. Koerner, J.W. Baur, Mechanical properties of printed epoxy-carbon fiber composites. Exp. Mech. **59**, 843–857 (2019). https://doi.org/10.1007/s11340-019-00498-z